

Search for Rare and Forbidden Charm Meson Decays $D^0 \rightarrow V\ell^+\ell^-$ and $h\ell\ell$

E. M. Aitala,⁹ S. Amato,¹ J. C. Anjos,¹ J. A. Appel,⁵ D. Ashery,¹⁴ S. Banerjee,⁵ I. Bediaga,¹ G. Blaylock,⁸ S. B. Bracker,¹⁵ P. R. Burchat,¹³ R. A. Burnstein,⁶ T. Carter,⁵ H. S. Carvalho,¹ N. K. Copty,¹² L. M. Cremaldi,⁹ C. Darling,¹⁸ K. Denisenko,⁵ S. Devmal,³ A. Fernandez,¹¹ G. F. Fox,¹² P. Gagnon,² C. Gobel,¹ K. Gounder,⁹ A. M. Halling,⁵ G. Herrera,⁴ G. Hurvits,¹⁴ C. James,⁵ P. A. Kasper,⁶ S. Kwan,⁵ D. C. Langs,¹² J. Leslie,² B. Lundberg,⁵ J. Magnin,¹ S. MayTal-Beck,¹⁴ B. Meadows,³ J. R. T. de Mello Neto,¹ D. Mihalcea,⁷ R. H. Milburn,¹⁶ J. M. de Miranda,¹ A. Napier,¹⁶ A. Nguyen,⁷ A. B. d’Oliveira,^{3,11} K. O’Shaughnessy,² K. C. Peng,⁶ L. P. Perera,³ M. V. Purohit,¹² B. Quinn,⁹ S. Radeztsky,¹⁷ A. Rafatian,⁹ N. W. Reay,⁷ J. J. Reidy,⁹ A. C. dos Reis,¹ H. A. Rubin,⁶ D. A. Sanders,⁹ A. K. S. Santha,³ A. F. S. Santoro,¹ A. J. Schwartz,³ M. Sheaff,¹⁷ R. A. Sidwell,⁷ A. J. Slaughter,¹⁸ M. D. Sokoloff,³ J. Solano,¹ N. R. Stanton,⁷ R. J. Stefanski,⁵ K. Stenson,¹⁷ D. J. Summers,⁹ S. Takach,¹⁸ K. Thorne,⁵ A. K. Tripathi,⁷ S. Watanabe,¹⁷ R. Weiss-Babai,¹⁴ J. Wiener,¹⁰ N. Witchey,⁷ E. Wolin,¹⁸ S. M. Yang,⁷ D. Yi,⁹ S. Yoshida,⁷ R. Zaliznyak,¹³ and C. Zhang⁷

(Fermilab E791 Collaboration)

¹ Centro Brasileiro de Pesquisas Físicas, Rio de Janeiro, Brazil

³ University of Cincinnati, Cincinnati, OH 45221

⁵ Fermilab, Batavia, IL 60510

⁷ Kansas State University, Manhattan, KS 66506

⁹ University of Mississippi-Oxford, University, MS 38677

¹¹ Universidad Autonoma de Puebla, Puebla, Mexico

¹³ Stanford University, Stanford, CA 94305

¹⁵ Box 1290, Enderby, British Columbia V0E 1V0, Canada

¹⁷ University of Wisconsin, Madison, WI 53706

² University of California, Santa Cruz, CA 95064

⁴ CINVESTAV, 07000 Mexico City, DF Mexico

⁶ Illinois Institute of Technology, Chicago, IL 60616

⁸ University of Massachusetts, Amherst, MA 01003

¹⁰ Princeton University, Princeton, NJ 08544

¹² University of South Carolina, Columbia, SC 29208

¹⁴ Tel Aviv University, Tel Aviv, Israel

¹⁶ Tufts University, Medford, MA 02155

¹⁸ Yale University, New Haven, CT 06511

(November 1, 2018)

We report results of a search for flavor-changing neutral current (FCNC), lepton-flavor, and lepton-number violating decays of the D^0 (and its antiparticle) into 3 and 4-bodies. Using data from Fermilab charm hadroproduction experiment E791, we examine modes with two leptons (muons or electrons) and either a ρ^0 , \overline{K}^{*0} , or ϕ vector meson or a non-resonant $\pi\pi$, $K\pi$, or KK pair of pseudoscalar mesons. No evidence for any of these decays is found. Therefore, we present branching-fraction upper limits at 90% confidence level for the 27 decay modes examined (18 new).

PACS numbers: 11.30.Fs, 12.15.Mm, 13.20.Fc, 14.80.Cp

The E791 Collaboration has previously reported limits on rare and forbidden dilepton decays of the charged charm D meson [1,2]. Such measurements probe the $SU(2) \times U(1)$ Standard Model of electroweak interactions in search of new mediators and couplings [3,4]. We extend the methodology to 27 dilepton decay modes of the neutral D meson. The modes are resonant $D^0 \rightarrow V\ell^+\ell^-$ decays, where V is a ρ^0 , \overline{K}^{*0} , or ϕ , and non-resonant $D^0 \rightarrow h\ell\ell$ decays, where h is a π or K . The leptons are either muons or electrons. Charge-conjugate modes are implied. The modes are lepton flavor-violating (e.g., $D^0 \rightarrow \rho^0\mu^+e^-$), or lepton number-violating (e.g., $D^0 \rightarrow \pi^-\pi^-\mu^+\mu^+$), or flavor-changing neutral current decays (e.g., $D^0 \rightarrow \overline{K}^{*0}e^+e^-$). Box diagrams can mimic FCNC decays, but only at the 10^{-10} to 10^{-9} level [4,5]. Long range effects (e.g., $D^0 \rightarrow \overline{K}^{*0}\rho^0$, $\rho^0 \rightarrow e^+e^-$) can occur at the 10^{-6} level [5,6]. Numerous experiments have studied rare decays of charge -1/3 strange quarks. Charge 2/3 charm quarks are interesting because they might couple differently [7].

The data come from measurements with the Fermilab E791 spectrometer [8]. A total of 2×10^{10} events were taken with a loose transverse energy requirement. These events were produced by a $500 \text{ GeV}/c \pi^-$ beam interacting in a fixed target consisting of five thin, well-separated foils. Track and vertex information came from “hits” in 23 silicon microstrip planes and 45 wire chamber planes. This information and the bending provided by two dipole magnets were used for momentum analysis of charged particles. Kaon identification was carried out by two multi-cell Čerenkov counters that provided π/K separation in the momentum range $6 - 60 \text{ GeV}/c$ [9]. We required that the momentum-dependent light yield in the Čerenkov counters be consistent for kaon-candidate tracks, except for those in decays with $\phi \rightarrow K^+K^-$, where the narrow mass window for the ϕ decay provided sufficient kaon identification (ID).

Electron ID was based on transverse shower shape plus matching wire chamber tracks to shower positions and energies in an electromagnetic calorimeter [10]. The elec-

tron ID efficiency varied from 62% below 9 GeV/c to 45% above 20 GeV/c . The probability to misidentify a pion as an electron was $\sim 0.8\%$, independent of pion momentum.

Muon ID was obtained from two planes of scintillation counters. The first plane (5.5 m \times 3.0 m) of 15 counters measured the horizontal position while the second plane (3.0 m \times 2.2 m) of 16 counters measured the vertical position. There were about 15 interaction lengths of shielding upstream of the counters to filter out hadrons. Data from $D^+ \rightarrow \overline{K}^{*0} \mu^+ \nu_\mu$ decays [11] were used to choose selection criteria for muon candidates. Timing information from the smaller set of muon scintillation counters was used to improve the horizontal position resolution. Counter efficiencies, measured using muons originating from the primary target, were found to be $(99 \pm 1)\%$ for the smaller counters and $(69 \pm 3)\%$ for the larger counters. The probability for misidentifying a pion as a muon decreased with momentum, from about 6% at 8 GeV/c to $(1.3 \pm 0.1)\%$ above 20 GeV/c .

Events with evidence of well-separated production (primary) and decay (secondary) vertices were selected to separate charm candidates from background. Secondary vertices were required to be separated from the primary vertex by greater than $12 \sigma_L$, where σ_L is the calculated resolution of the measured longitudinal separation. Also, the secondary vertex had to be separated from the closest material in the target foils by greater than $5 \sigma'_L$, where σ'_L is the uncertainty in this separation. The vector sum of the momenta from secondary vertex tracks was required to pass within 40 μm of the primary vertex in the plane perpendicular to the beam. Finally, the net momentum of the charm candidate transverse to the line connecting the production and decay vertices had to be less than 300 MeV/c . Decay track candidates were required to pass approximately 10 times closer to the secondary vertex than to the primary vertex. These selection criteria and kaon identification requirements were the same for both the search mode and for its normalization signal (discussed below). The mass ranges used for the resonant masses were: $|m_{\pi^+\pi^-} - m_{\rho^0}| < 150 \text{ MeV}/c^2$, $|m_{K^-\pi^+} - m_{\overline{K}^{*0}}| < 55 \text{ MeV}/c^2$, and $|m_{K^+K^-} - m_\phi| < 10 \text{ MeV}/c^2$.

To determine our selection cuts we used a “blind” analysis technique. Before the selection criteria were finalized, all events having masses within a window ΔM_S around the mass of the D^0 were “masked” so that the presence or absence of any potential signal candidates would not bias our choice of selection criteria. All criteria were then chosen by studying events generated by a Monte Carlo (MC) simulation program and background events, outside the signal windows, from real data. The criteria were chosen to maximize the ratio $N_{MC}/\sqrt{N_B}$, where N_{MC} and N_B are the numbers of MC and background events, respectively, after all selection criteria were applied. The data within the signal windows were

unmasked only after this optimization. We used asymmetric windows for the decay modes containing electrons to allow for the bremsstrahlung low-energy tail. The signal windows were: $1.83 < M(D^0) < 1.90 \text{ GeV}/c^2$ for $\mu\mu$ and $1.76 < M(D^0) < 1.90 \text{ GeV}/c^2$ for ee and μe modes.

We normalize the sensitivity of our search to topologically similar hadronic 3-body (resonant) or 4-body (non-resonant) decays. One exception to this is the case of $D^0 \rightarrow \rho^0 \ell^\pm \ell^\mp$ where we normalize to nonresonant $D^0 \rightarrow \pi^+\pi^-\pi^+\pi^-$ because there is no published branching fraction for $D^0 \rightarrow \rho^0 \pi^+\pi^-$. Table I lists the normalization mode used for each signal mode and the fitted number of data events (N_{Norm}).

The upper limit for each branching fraction B_X is calculated using the following formulae:

$$B_X = \frac{N_X}{N_{\text{Norm}}} \frac{\varepsilon_{\text{Norm}}}{\varepsilon_X} \times B_{\text{Norm}}, \quad \frac{\varepsilon_{\text{Norm}}}{\varepsilon_X} = \frac{f_{\text{Norm}}^{\text{MC}}}{f_X^{\text{MC}}}. \quad (1)$$

N_X is the 90% confidence level (CL) upper limit on the number of decays for the rare or forbidden decay mode X and B_{Norm} is the normalization mode branching fraction obtained from the Particle Data Group [12]. $\varepsilon_{\text{Norm}}$ and ε_X are the detection efficiencies while $f_{\text{Norm}}^{\text{MC}}$ and f_X^{MC} are the fractions of Monte Carlo events that are reconstructed and pass the final selection criteria, for the normalization and decay modes respectively.

TABLE I. Normalization modes used.

Decay Mode	Normalization Mode	N_{Norm}
$D^0 \rightarrow \rho^0 \ell^\pm \ell^\mp$	$D^0 \rightarrow \pi^+\pi^-\pi^+\pi^-$	2049 ± 53
$D^0 \rightarrow \overline{K}^{*0} \ell^\pm \ell^\mp$	$D^0 \rightarrow \overline{K}^{*0} \pi^+\pi^-$	5451 ± 72
$D^0 \rightarrow \phi \ell^\pm \ell^\mp$	$D^0 \rightarrow \phi \pi^+\pi^-$	113 ± 19
$D^0 \rightarrow \pi\pi\ell\ell$	$D^0 \rightarrow \pi^+\pi^-\pi^+\pi^-$	2049 ± 53
$D^0 \rightarrow K\pi\ell\ell$	$D^0 \rightarrow K^-\pi^+\pi^-\pi^+$	11550 ± 113
$D^0 \rightarrow KK\ell\ell$	$D^0 \rightarrow K^+K^-\pi^+\pi^-$	406 ± 41

The MC simulations use PYTHIA/JETSET [13] as the physics generator and model the effects of resolution, detector geometry, magnetic fields, multiple scattering, interactions in the detector material, detector efficiencies, and the analysis selection criteria. The efficiencies for the normalization modes varied from approximately 0.2% to 1% depending on the mode, and the efficiencies for the search modes varied from approximately 0.05% to 0.34%. We take muon and electron ID efficiencies from data.

Monte Carlo studies show that the experiment’s acceptances are nearly uniform across the Dalitz plots, except that the dilepton identification efficiencies typically drop to near zero at the dilepton mass threshold. While the loss in efficiency varies channel by channel, the efficiency typically reaches its full value at masses only a few hundred MeV/c^2 above the dilepton mass threshold. We use a constant weak-decay matrix element when calculating the overall detection efficiencies.

The 90% CL upper limits N_X are calculated using the method of Feldman and Cousins [14] to account for background, and then corrected for systematic errors by the method of Cousins and Highland [14]. In these methods, the numbers of signal events are determined by simple counting, not by a fit. All results are shown in Fig. 1 and listed in Table II. Upper limits are determined using the number of candidate events observed and expected number of background events within the signal region.

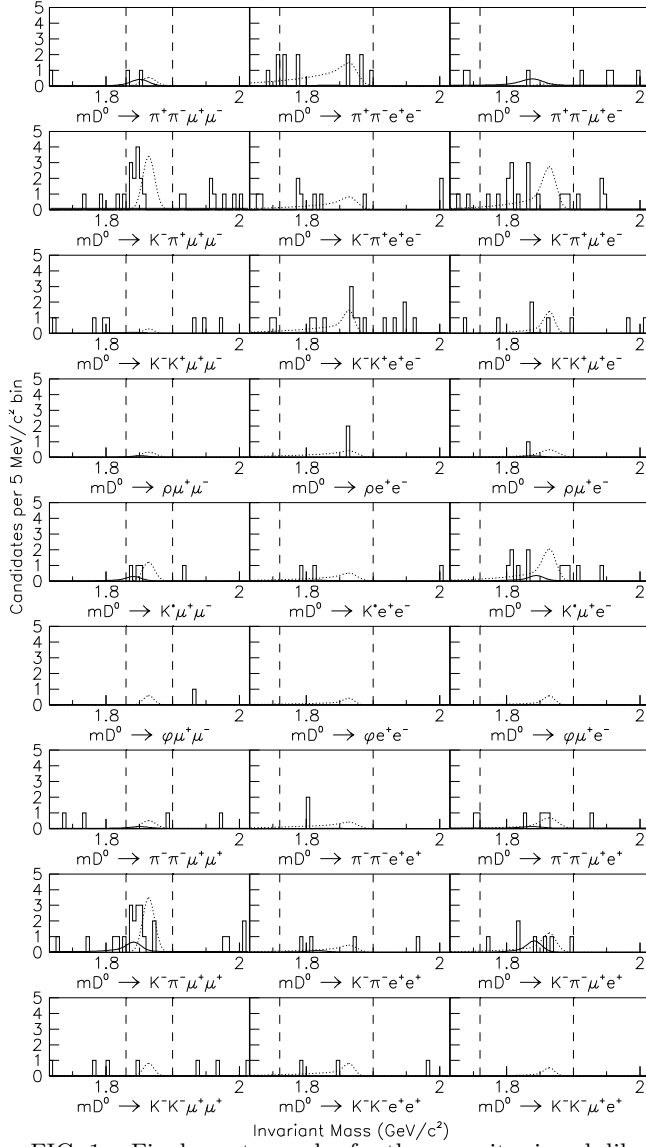


FIG. 1. Final event samples for the opposite signed dilepton (rows 1–3), resonant (rows 4–6), and same signed dilepton modes (rows 7–9) of D^0 decays. The solid curves display total estimated background; the dotted curves display signal shape for a number of events equal to the 90% CL upper limit. The dashed vertical lines are the ΔM_S boundaries.

Background sources that are not removed by the selection criteria discussed earlier include decays in which hadrons (from real, fully-hadronic decay vertices) are misidentified as leptons. These misidentified leptons can

come from hadronic showers reaching muon counters, decays-in-flight, and random overlaps of tracks from otherwise separate decays (“accidental” sources). In the case where kaons are misidentified as pions or leptons, candidate masses shift below signal windows. However, we remove these events to prevent them from influencing our background estimate, which is partially obtained from the mass sidebands (see discussion of N_{Cmb} below). To remove these events prior to the selection-criteria optimization, we reconstruct all candidates as each of the non-resonant normalization modes and test whether the masses are consistent with m_{D^0} . If so, we remove the events, but only if the number of kaons in the final state differs from that of the search mode. We do not remove events having the same number of kaons, as the loss in acceptance for true signal events would be excessive.

There remain two sources of background: hadronic decays where pions are misidentified as leptons (N_{MisID}) and “combinatorial” background (N_{Cmb}) arising primarily from false vertices and partially reconstructed charm decays. The background N_{MisID} arises from the normalization modes. To estimate the rate for misidentifying $\pi\pi$ as $\ell\ell$, for all but the $D^0 \rightarrow K^-\pi^+\ell^+\ell^-$ modes, we assume all $D^0 \rightarrow K^-\pi^+\ell^+\ell^-$ candidates observed (after subtracting combinatoric background estimated from mass sidebands) result from misidentification of $D^0 \rightarrow K^-\pi^+\pi^-\pi^+$ decays and count the number of $D^0 \rightarrow K^-\pi^+\ell^+\ell^-$ decays passing the final selection criteria. We then divide by twice the number of $D^0 \rightarrow K^-\pi^+\pi^-\pi^+$ normalization events with $K^-\pi^+\ell^+\ell^-$ mass within ΔM_S boundaries (twice because there are two possible π^+ misidentifications).

From this procedure, the following misidentification rates were obtained: $r_{\mu\mu} = (3.4 \pm 2.4) \times 10^{-4}$, $r_{\mu e} = (4.2 \pm 1.4) \times 10^{-4}$, and $r_{ee} = (9.0 \pm 6.2) \times 10^{-5}$. For modes in which two possible pion combinations can contribute, e.g., $D^0 \rightarrow K^-\pi^+\mu^\pm\mu^\mp$, we use twice the above rate; and for $D^0 \rightarrow \pi^+\pi^-\pi^+\pi^-$, where there are 4 possible combinations, we use 4 times this rate in calculating $D^0 \rightarrow \pi^+\pi^-\ell^+\ell^-$. Using these rates, we estimate the numbers of misidentified candidates, $N_{\text{MisID}}^{V\ell\ell}$ and $N_{\text{MisID}}^{hh\ell\ell}$, in the signal windows as follows:

$$N_{\text{MisID}}^{hh\ell\ell} = r_{ee} \times N_{\text{Norm}}^{hh\pi\pi} \text{ and } N_{\text{MisID}}^{V\ell\ell} = r_{ee} \times N_{\text{Norm}}^{V\pi\pi}, \quad (2)$$

where $N_{\text{Norm}}^{hh\pi\pi}$ and $N_{\text{Norm}}^{V\pi\pi}$ are the numbers of normalization hadronic decay candidates in the signal windows.

To calculate the upper limits for the $D^0 \rightarrow K^-\pi^+\ell^+\ell^-$ modes, we set N_{MisID} to zero as we do not have an independent estimate of the misidentification rates. This results in conservative upper limits. If we had used the misidentification rates from our previous, 3-body decay study [2], then our limits for the three $D^0 \rightarrow K^-\pi^+\ell^+\ell^-$ modes would be lower by about a factor of two.

To estimate the combinatoric background N_{Cmb} within a signal window ΔM_S , we count events having masses within an adjacent background mass win-

dow ΔM_B , and scale this number ($N_{\Delta M_B}$) by the relative sizes of these windows: $N_{\text{Cmb}} = (\Delta M_S / \Delta M_B) \times N_{\Delta M_B}$. To be conservative in calculating our 90% confidence level upper limits, we take combinatoric backgrounds to be zero when no events are located above the mass windows. Table II shows the numbers of combinatoric background, misidentification background, and observed events for all 27 modes.

TABLE II. E791 90% confidence level (CL) upper limits on the number of events and branching fraction limits ($\times 10^{-5}$). Previously published limits [12,15] for the nine $D^0 \rightarrow V\ell^+\ell^-$ modes are 23, 10, 4.9, 118, 14, 10, 41, 5.2, and 3.4×10^{-5} .

Mode	(Est. BG)		Sys.	E791		
$D^0 \rightarrow$	N_{Cmb}	N_{MisID}	N_{Obs}	Err.	N_X	Limit
$\pi^+\pi^-\mu^+\mu^-$	0.00	3.16	2	11%	2.96	3.0
$\pi^+\pi^+e^+e^-$	0.00	0.73	9	12%	15.2	37.3
$\pi^+\pi^-\mu^\pm e^\mp$	5.25	3.46	1	15%	1.06	1.5
$K^-\pi^+\mu^+\mu^-$	3.65	0.00	12	11%	15.4	35.9
$K^-\pi^+e^+e^-$	3.50	0.00	6	15%	7.53	38.5
$K^-\pi^+\mu^\pm e^\mp$	5.25	0.00	15	12%	17.3	55.3
$K^+K^-\mu^+\mu^-$	2.13	0.17	0	17%	1.22	3.3
$K^+K^-e^+e^-$	6.13	0.04	9	18%	9.61	31.5
$K^+K^-\mu^\pm e^\mp$	3.50	0.17	5	17%	6.61	18
$\rho^0\mu^+\mu^-$	0.00	0.75	0	10%	1.80	2.2
$\rho^0e^+e^-$	0.00	0.18	1	12%	4.28	12.4
$\rho^0\mu^\pm e^\mp$	0.00	0.82	1	11%	3.60	6.6
$\overline{K}^{*0}\mu^+\mu^-$	0.30	1.87	3	24%	5.40	2.4
$\overline{K}^{*0}e^+e^-$	0.88	0.49	2	25%	4.68	4.7
$\overline{K}^{*0}\mu^\pm e^\mp$	1.75	2.30	9	24%	12.8	8.3
$\phi\mu^+\mu^-$	0.30	0.04	0	33%	2.33	3.1
ϕe^+e^-	0.00	0.01	0	33%	2.75	5.9
$\phi\mu^\pm e^\mp$	0.00	0.05	0	33%	2.71	4.7
$\pi^-\pi^-\mu^+\mu^+$	0.91	0.79	1	9%	2.78	2.9
$\pi^-\pi^-e^+e^+$	0.00	0.18	1	11%	4.26	11.2
$\pi^-\pi^-\mu^+e^+$	2.63	0.86	4	10%	5.18	7.9
$K^-\pi^-\mu^+\mu^+$	2.74	3.96	14	9%	15.7	39.0
$K^-\pi^-e^+e^+$	0.88	1.04	2	16%	4.14	20.6
$K^-\pi^-\mu^+e^+$	0.00	4.88	7	11%	7.81	21.8
$K^-K^-\mu^+\mu^+$	1.22	0.00	1	17%	3.27	9.4
$K^-K^-e^+e^+$	0.88	0.00	2	17%	5.28	15.2
$K^-K^-\mu^+e^+$	0.00	0.00	0	17%	2.52	5.7

The sources of systematic errors in this analysis include: errors from the fit to the normalization sample N_{Norm} ; statistical uncertainty on the selection efficiencies, calculated for Monte Carlo simulated events, for both $f_{\text{Norm}}^{\text{MC}}$ and f_X^{MC} ; uncertainties in the calculation of misidentification background; and uncertainties in the relative efficiency for each mode, including lepton tagging efficiencies. These tagging efficiency uncertainties include: 1) muon counter efficiencies from hardware performance; and 2) the fraction of signal events (based on simulations) that would remain outside the signal window due to bremsstrahlung tails. Also, for the $D^0 \rightarrow \rho^0\ell^+\ell^+$ modes, an additional systematic error is included because we are using $D^0 \rightarrow \pi^+\pi^-\pi^+\pi^-$ as the

normalization mode since there is no published branching fraction for $D^0 \rightarrow \rho^0\pi^+\pi^-$. The sums, taken in quadrature, of these systematic errors are listed in Table II.

In summary, we use a “blind” analysis of data from Fermilab experiment E791 to obtain upper limits on the dilepton branching fractions for 27 flavor-changing neutral current, lepton-number violating, and lepton-family violating decays of D^0 mesons. No evidence for any of these 3 and 4-body decays is found. Therefore, we present upper limits on the branching fractions at the 90% confidence level. Four limits represent significant improvements over previously published results. Eighteen of these modes have no previously reported limits.

We thank the staffs of Fermilab and participating institutions. This research was supported by the Brazilian Conselho Nacional de Desenvolvimento Científico e Tecnológico, CONACyT (Mexico), the Israeli Academy of Sciences and Humanities, the U.S.-Israel Binational Science Foundation, and the U.S. National Science Foundation and Dept. of Energy. The Universities Research Assn. operates Fermilab for the U.S. Dept. of Energy.

- [1] E. M. Aitala *et al.*, Phys. Rev. Lett. **76**, 364 (1996).
- [2] E. M. Aitala *et al.*, Phys. Lett. **B462**, 401 (1999).
- [3] See for example: S. Pakvasa, hep-ph/9705397; S. Pakvasa, Chin. J. Phys. (Taipei) **32**, 1163 (1994); D. A. Sanders, Mod. Phys. Lett. **A15**, 1399 (2000).
- [4] A. J. Schwartz, Mod. Phys. Lett. **A8**, 967 (1993).
- [5] S. Fajfer, S. Prelovšek, and P. Singer, Phys. Rev. D **58**, 094038 (1998); S. Prelovšek, hep-ph/0010106.
- [6] P. Singer, Acta Phys. Polon. **B30**, 3861 (1999); P. Singer and D.-X. Zhang, Phys. Rev. D **55**, 1127 (1997).
- [7] G. López Castro, R. Martínez, and J. H. Muñoz, Phys. Rev. D **58**, 033003 (1998).
- [8] J. A. Appel, Ann. Rev. Nucl. Part. Sci. **42** (1992) 367; D. J. Summers *et al.*, hep-ex/0009015; S. Amato *et al.*, Nucl. Instrum. Meth. **A324**, 535 (1993); S. Bracker *et al.*, IEEE Trans. Nucl. Sci. **43**, 2457 (1996); E. M. Aitala *et al.*, Eur. Phys. J. direct C **4**, 1 (1999).
- [9] D. Bartlett *et al.*, Nucl. Instrum. Meth. **A260**, 55 (1987).
- [10] V. K. Bharadwaj *et al.*, Nucl. Instrum. Meth. **155**, 411 (1978); *ibid.*, **A228**, 283 (1985); D. Summers, *ibid.*, 290.
- [11] E. M. Aitala *et al.*, Phys. Lett. **B440**, 435 (1998).
- [12] Particle Data Group, D. E. Groom *et al.*, Eur. Phys. J. C **15**, 1 (2000).
- [13] H.-U. Bengtsson and T. Sjöstrand, Comp. Phys. Comm. **82**, 74 (1994); T. Sjöstrand, hep-ph/9508391.
- [14] G. J. Feldman and R. D. Cousins, Phys. Rev. D **57**, 3873 (1998); R. D. Cousins and V. L. Highland, Nucl. Instrum. Meth. **A320**, 331 (1992).
- [15] CLEO Collaboration, A. Freyberger *et al.*, Phys. Rev. Lett. **76**, 3065 (1996); Fermilab E653 Collaboration, K. Kodama *et al.*, Phys. Lett. **B345**, 85 (1995).